2-15-1998

Deconvolving the information from an imperfect spherical gravitational-wave antenna

S. M. Merkowitz
Louisiana State University

W. W. Johnson
Louisiana State University

Recommended Citation

Merkowitz, S., & Johnson, W. (1998). Deconvolving the information from an imperfect spherical gravitational-wave antenna. *Europhysics Letters, 41* (4), 355-360. https://doi.org/10.1209/epl/i1998-00156-5

Deconvolving the information from an imperfect spherical gravitational wave antenna

Stephen M. Merkowitz* and Warren W. Johnson
Department of Physics and Astronomy, Louisiana State University, Baton Rouge, Louisiana 70803
(January 9, 1998)

We have studied the effects of imperfections in spherical gravitational wave antenna on our ability to properly interpret the data it will produce. The results of a numerical simulation are reported that quantitatively describe the systematic errors resulting from imperfections in various components of the antenna. In addition, the results of measurements on a room-temperature prototype are presented that verify it is possible to accurately deconvolve the data in practice.

PACS numbers: 04.80.Nn, 95.55.Ym

A spherical gravitational wave antenna was first proposed by Forward in 1971 [1]. The large cross section and the ability to determine the direction of a gravitational wave have been known for some time [2], but it was not until recently that its potential advantages have been actively studied [3–5]. For the past few years, several groups have been researching the possibility of constructing large scale spherical antennas [6].

To realize the full potential of these detectors, we must first be able to understand their behavior and properly interpret the data they will produce. The technique needed will depend on the particular type and arrangement of sensors used to detect the motions of the sphere. We have proposed and investigated the "truncated icosahedral" (TI) arrangement [3] for six identical radial motion resonant transducers. We have shown that this arrangement on a perfect sphere, but with equally noisy transducers, has the property that all five quadrupole components of the gravitational strain tensor are measured with equal sensitivity [7]. Other arrangements of transducers have been proposed [8,9], but most of them do not share this property [10].

The TI model, also called a truncated icosahedral gravitational wave antenna (TIGA), has been criticized on the basis that normal (small) imperfections will break the perfect symmetry, possibly having drastic effects on such a degenerate system, thereby making it difficult to extract the desired information from the data. We report here the theoretical and experimental results of an investigation into the effects of imperfections in a spherical antenna that refutes these criticisms and shows that the symmetry breaking can be easily handled.

The normal modes of an uncoupled elastic sphere can be described by the spacial eigenfunctions $\vec{\Psi}_{n\ell m}(r,\theta,\phi)$ (functions of the spherical harmonics) and the purely time dependent mode amplitudes $a_{n\ell m}(t)$ [7,11,12]. In general relativity only the $\ell = 2$ quadrupole modes strongly interact with a gravitational wave so for the remainder of this discussion we will assume $n = 1$, $\ell = 2$ and drop these subscripts from our notation. We denote the orientation of the 5 quadrupole modes relative to the lab frame by 2 Euler angles β_m and γ_m. If the quadrupole modes are degenerate these angles are arbitrary (restricted only by orthogonality of the modes). Imperfections of the sphere can lift the degeneracy causing the modes to "fix" themselves in a particular orientation. This effect has been shown to be the main result of symmetry breaking in an *uncoupled* sphere; the "shape" of the quadrupole mode remains mostly unchanged [13,14].

We consider that a number of small resonant transducers, with index $j = 1 \ldots J$, are added to the surface of the sphere to mechanically transform the small motion of the surface into a large motion of the resonator. We assume the resonators are constructed to obey a one-dimensional harmonic oscillator equation. The particular arrangement of resonators is indicated by their locations (θ_j, ϕ_j) on the sphere surface and their coupling to the surface motion in different directions $\vec{\epsilon}_j$. In the case of ideal radial resonators we would set $\vec{\epsilon}_j = \hat{r}$. The relative amount of surface displacement coupled to each resonator for a particular mode is specified by a "pattern matrix" defined as

$$B_{mj} \equiv \frac{1}{\alpha}\vec{\epsilon}_j \cdot \vec{\Psi}_m(R,\theta_j,\phi_j), \tag{1}$$

where α depends on the material and the radius R of the sphere [2,7]. Again, we assume that the transducers strongly interact only with the quadrupole modes of the sphere, which is appropriate if the mass of a resonator is small compared to the mass of the sphere [8,15].

The complete set of coupled equations of motion for the sphere and resonators can now be written [16]

$$\begin{bmatrix} \boldsymbol{M}^s & \boldsymbol{0} \\ \alpha \boldsymbol{M}^r \boldsymbol{B}^T & \boldsymbol{M}^r \end{bmatrix} \begin{bmatrix} \ddot{\boldsymbol{a}}(t) \\ \ddot{\boldsymbol{q}}(t) \end{bmatrix} + \begin{bmatrix} \boldsymbol{K}^s & -\alpha \boldsymbol{B}\,\boldsymbol{K}^r \\ \boldsymbol{0} & \boldsymbol{K}^r \end{bmatrix} \begin{bmatrix} \boldsymbol{a}(t) \\ \boldsymbol{q}(t) \end{bmatrix} = \begin{bmatrix} \boldsymbol{I} & -\alpha \boldsymbol{B} \\ \boldsymbol{0} & \boldsymbol{I} \end{bmatrix} \boldsymbol{f}(t), \tag{2}$$

*Present affiliation INFN-Laboratori Nazionali di Frascati, Via Enrico Fermi 40, I-00044 Frascati (Roma), ITALY

where we have defined 4 diagonal matrices whose elements are the mass m and spring constants k of both the sphere modes (superscript s) and the resonators (superscript r),

$$M^s_{jm} \equiv \delta_{jm} m^s_m, \quad M^r_{jm} \equiv \delta_{jm} m^r_j, \quad K^s_{jm} \equiv \delta_{jm} k^s_m, \quad K^r_{jm} \equiv \delta_{jm} k^r_j. \tag{3}$$

The column vector $\boldsymbol{a}$ has five components, one for each sphere mode amplitude, and has a one-to-one correspondence with the quadrupole components of the gravitational wave strain tensor [7,12]. The column vector $\boldsymbol{q}$ has J components, one for each resonator displacement, and are the observable quantity. The column vector $\boldsymbol{f}$ contains any forces (such as a gravitational wave) acting on the sphere and resonators.

A normal mode solution of these coupled equations is possible using standard techniques [16]. We find the response of the normal modes $\boldsymbol{\eta}(\omega)$ to any external forces, including gravitational waves, is given by

$$\boldsymbol{\eta}(\omega) = \boldsymbol{G}(\omega)\boldsymbol{V}^{-1} \begin{bmatrix} \boldsymbol{M}^s & \boldsymbol{0} \\ \alpha \boldsymbol{M}^r \boldsymbol{B}^T & \boldsymbol{M}^r \end{bmatrix}^{-1} \begin{bmatrix} \boldsymbol{I} & -\alpha \boldsymbol{B} \\ \boldsymbol{0} & \boldsymbol{I} \end{bmatrix} \boldsymbol{f}(\omega). \tag{4}$$

The matrix $\boldsymbol{V}$ is constructed from the eigenvectors of the normal modes, and the matrix $\boldsymbol{G}(\omega)$ is constructed from their eigenvalues. The matrix $\boldsymbol{V}$ can also be used to return to the original sphere and resonator coordinates

$$\begin{bmatrix} \boldsymbol{a}(\omega) \\ \boldsymbol{q}(\omega) \end{bmatrix} = \boldsymbol{V}\, \boldsymbol{\eta}(\omega). \tag{5}$$

$\boldsymbol{V}$ is always invertible thus it is possible to use the inverse of Eq. (5) to transform the data to normal coordinates where the frequency response is simple.

Examining Eqs. (4) and (5), we see that in order to obtain all the information about an excitation we must have knowledge of both the sphere $\boldsymbol{a}$ and resonator $\boldsymbol{q}$ modes even though only the resonator motion is observable. A simple solution emerges if we limit ourselves to the case of "close" to the TI arrangement (six radial resonators placed at the center of six non-antipodal pentagon faces of an imaginary TI concentric to the sphere). The eigenfunctions of an ideal TIGA are such that the motion of the resonators mimic the ellipsoidal (quadrupole) deformation of the sphere's surface either in phase or anti-phase [7]. We can picture the collective motion of the six resonators to describe six "resonator ellipsoids", five of which are mimicking the "quadrupole ellipsoids" of the sphere (the sixth resonator ellipsoid is just a "breathing" sphere: the six resonators are moving in unison with equal amplitude and the sphere surface does not move at all). Each individual resonator displacement q_j represents a superposition of the point radial deformation of the six resonator ellipsoids at a particular location. The transformation between point radial deformations $\boldsymbol{q}$ and ellipsoidal amplitudes $\boldsymbol{g}$ is given by the pattern matrix $\boldsymbol{B}$:

$$\boldsymbol{g} = \boldsymbol{B}\, \boldsymbol{q}. \tag{6}$$

The resonator ellipsoids $\boldsymbol{g}$ are proportional to the sphere modes $\boldsymbol{a}$ so we sometimes refer to them as "mode channels." We also point out that Eq. (6) can be seen as a linear coordinate transformation between the measured point radial displacement and a 5-dimensional abstract vector space based on the spherical harmonics that has a one-to-one correspondence with the five quadrupole components of the gravitational strain tensor [7,15]. While not unique to TIGA, such a simple transformation is not possible for most other arrangements of transducers.

We are now prepared to discuss how imperfections effect our ability to deconvolve the signal from the transducers. One source of error is the resonator ellipsoids may be deformed so that they no longer mimic the sphere surface. This could lead to errors in calculating both the matrix $\boldsymbol{V}$ and the mode channels $\boldsymbol{g}$. Another source of error is the uncertainty of the values of all the system parameters. Most of the parameters can be measured, either directly or indirectly, but we will be limited by the accuracy of that measurement.

The transformation matrix $\boldsymbol{V}$ can be measured by applying a continuous sinusoidal force anywhere on the sphere's surface at the frequency of one of the normal modes. (Note that this technique requires the normal modes to be *non-degenerate*, thus it is actually preferable to have a small amount of symmetry breaking.) The frequency response of the resonators will be simple because they are being driven at a single frequency. From Eq. (5) we see that the amplitude and phase of their response make up a single column of $\boldsymbol{V}$. By exciting each normal mode in turn, the complete $\boldsymbol{V}$ matrix can be measured. The only assumption made in calculating $\boldsymbol{V}$ is that the resonators are "close" to the TI arrangement so that an ideal pattern matrix $\boldsymbol{B}$ can be used and the sphere modes $\boldsymbol{a}$ can be replaced by the mode channels $\boldsymbol{g}$.

The quadrupole mode orientation angles β_m and γ_m can be measured directly only before the resonant transducers are attached [13]. This is also true for the the mass of the resonators m^r_j and the sphere modes m^s_m, and their respective spring constants k^r_j and k^s_m. Once the system is coupled together these parameters cannot be measured

independently. The positions of the resonators (θ_j, ϕ_j) can be easily measured, but precise values of their couplings $\vec{\epsilon}_j$ are much harder to determine.

We developed a numerical simulation of a TIGA that calculates the error associated with a measurement due to imperfections and asymmetries as well as our uncertainty of the precise values of the above parameters. We simulated a gravitational wave burst excitation of an imperfect TIGA and used the above analysis techniques to estimate the direction of the wave from the simulated output of the transducers. The analysis assumed parameter values of an ideal TIGA and a measured $\boldsymbol{V}$ matrix. The "real" (perturbed) parameters of the imperfect TIGA were calculated by adding uniformly distributed random numbers to the ideal values. The range of values of the random number was a fraction (tolerance) of the ideal value (2π for the angles).

The results of the simulation are shown in Fig. 1. Plotted is the solid angle estimation error $\Delta\Omega$ and the percentage error σ_h/h for estimating the strain amplitude for a range of tolerances. Parameters not shown had errors close or equal to zero. Because the tolerance is expressed as a percent of the ideal parameter values, varying the magnitude of the ideal parameters (for example doubling the mass of the sphere) produced identical results. Also varying the direction and polarization amplitudes of the gravitational wave produced similar results. From these results we conclude that the analysis becomes unreliable only after the tolerance of all the parameters exceeds about 3%. This is certainly an obtainable level of precision; one expects to set the tolerances on a real antenna to better than 1%.

Also shown in Fig. 1 are the errors due to a finite signal-to-noise ratio, calculated in a similar fashion to the analysis of Zhou and Michelson [9], but using the direction finding algorithm used in our measurements [13]. Note that this is a random error whereas the tolerance errors are systematic. Comparing the two sources of error, we find that one would need a signal-to-noise ratio of about 1000 in energy before the tolerance errors become significant. While one might hope to observe sources at this level, the most optimistic predictions lead to considerably smaller values [17].

To further evaluate the feasibility of a spherical antenna, we constructed a 0.8 m diameter, Aluminum alloy, room-temperature prototype TIGA [13,16]. Six radial resonant transducers were attached to the surface in the TI arrangement: placed at the center of each of the six lower pentagon faces. The response of each resonator was converted to an electrical signal by a piezoelectric strain gauge, whose output was recorded on a high speed data acquisition system. The apparatus is described in detail in Ref. [18].

Since no laboratory source of gravitational waves exists, we chose to apply an impulsive force to the surface of the prototype to test the developed techniques. To quantify the test, we checked if the location of the impulse could be measured from the response of the resonators.

We began by measuring the transformation matrix $\boldsymbol{V}$ as described above. Impulsive forces were then applied by sending a short electrical pulse to a piezoelectric shaker attached to the surface of the TI. The data from the transducers were recorded, transformed to normal coordinates, fit for phase and amplitude, and finally transformed to mode channels. From the mode channels the location of the impulse was calculated. The algorithm used to determine the location of the impulse can also be used to calculate the direction of a gravitational wave [13,16]. The results of this analysis for the various impulse locations is shown in Fig. 2. From these results, we conclude that it was possible to reconstruct the location of the impulses, within the accuracy of the experiment, without major difficulties.

In summary, from the numerical and experimental results we conclude that imperfections in a spherical antenna can be easily handled and that the error associated with the asymmetries are small. We find that the TI arrangement is fairly robust to these normal imperfections. The techniques for deconvolving the data are mostly linear algebra, making their implementation simple in an automated data analysis system. The measurement of the transformation matrix $\boldsymbol{V}$ takes into account most deviations from perfect symmetry and enables the data to be transformed to a space where the frequency complications can be easily handled. The algorithms were tested on the prototype TIGA and found to be consistent with the measured results. Finally, since all the techniques described and tested can be applied *in situ*, they are directly applicable for use on a real spherical antenna searching for gravitational waves.

We thank W. O. Hamilton for essential advice and support. This research was supported by the National Science Foundation under Grant No. PHY-9311731.

---

[1] R. Forward, Gen. Relativ. Gravit. **2**, 149 (1971).
[2] R. V. Wagoner and H. J. Paik, in *Proceedings of International Symposium on Experimental Gravitation, Pavia* (Roma Accademia Nazionale dei Lincei, Roma, 1976), pp. 257–265.
[3] W. W. Johnson and S. M. Merkowitz, Phys. Rev. Lett. **70**, 2367 (1993).
[4] E. Coccia, J. A. Lobo, and J. A. Ortega, Phys. Rev. D **52**, 3735 (1995).
[5] G. M. Harry, T. R. Stevenson, and H. J. Paik, Phys. Rev. D **54**, 2409 (1996).

[6] *Omnidirectional gravitational radiation observatory: Proceedings of the first international workshop*, edited by W. F. Velloso, O. D. Aguiar, and N. S. Magalhães (World Scientific, Singapore, 1997).
[7] S. M. Merkowitz and W. W. Johnson, Phys. Rev. D **51**, 2546 (1995).
[8] J. A. Lobo and M. A. Serrano, Europhys. Lett. **35**, 253 (1996).
[9] C. Zhou and P. F. Michelson, Phys. Rev. D **51**, 2517 (1995).
[10] T. R. Stevenson, Phys. Rev. D **56**, 564 (1997).
[11] N. Ashby and J. Dreitlein, Phys. Rev. D **12**, 336 (1975).
[12] J. A. Lobo, Phys. Rev. D **52**, 591 (1995).
[13] S. M. Merkowitz and W. W. Johnson, Phys. Rev. D **53**, 5377 (1996).
[14] E. Coccia *et al.*, Phys. Lett. A **219**, 263 (1996).
[15] J. A. Lobo and M. A. Serrano, Submitted to Phys. Rev. D.
[16] S. M. Merkowitz and W. W. Johnson, Phys. Rev. D **56**, 7513 (1997).
[17] L. S. Finn, in *Proceedings of the OMNI-1 workshop* [6].
[18] S. M. Merkowitz, Ph.D. thesis, Louisiana State University, 1995.

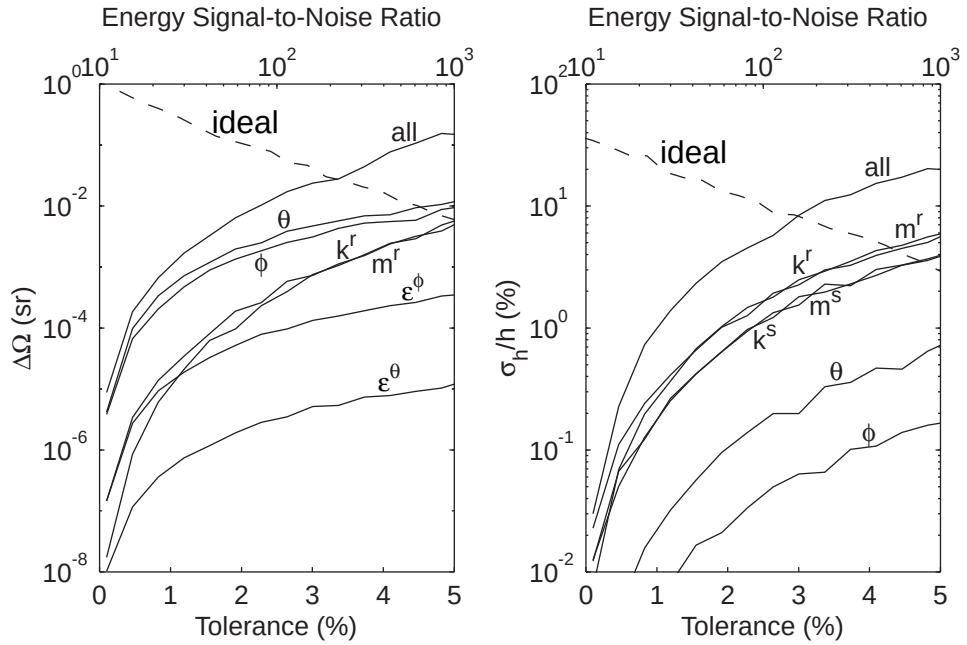

FIG. 1. The solid angle direction estimation error and the percentage error in estimating the strain magnitude as functions of the tolerance on the system parameters of a TIGA and as functions of the signal-to-noise ratio for an ideal TIGA. Each solid line corresponds to the bottom axis and represents the results of a 200 trial simulation with the indicated parameter varied within the corresponding tolerances. The dashed lines corresponds to the top axis and represents the results of a simulation of an ideal TIGA for a range of signal-to-noise ratios.

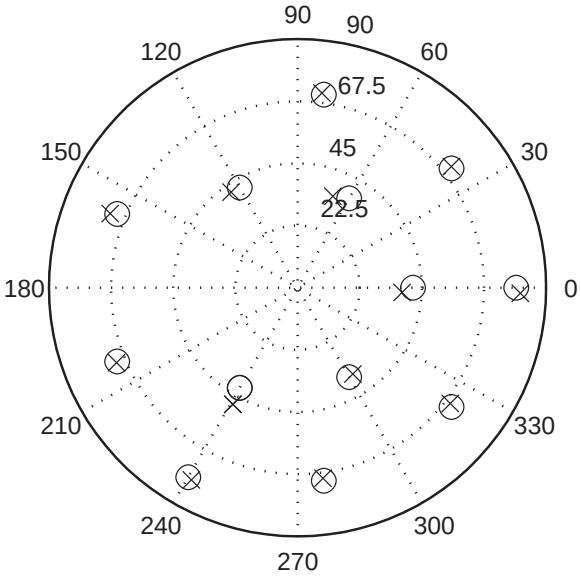

FIG. 2. Location of several impulses applied to the prototype TIGA. Each x marks the location calculated from the motion sensor data and the nearby o marks the location of the center of the shaker measured geometrically.